# 19F MR for drug delivery research

**X. Liu[1], Z-X. Jiang[2], Y. B. Yu[3], and E-K. Jeong[4]**

[1]University of Utah, Salt Lake City, Utah, United States, [2]Pharmaceutics & Pharmaceutical Chemistry, University of Utah, Salt Lake City, Utah, United States, [3]Bioengineering, University of Maryland, College Park, Maryland, United States, [4]Radiology, University of Utah, Salt Lake City, Utah, United States

**Introduction:** $^{1}$H MR imaging of water protons in tissue is widely used for studying the pharmacokinetics of Gd-chelate based endogenous contrast agent. The concentration of the delivered compound is indirectly measured by analyzing the change in the proton MRI signal intensity. The introduction of the Gd-chelate based agent induces the change in proton MR relaxation times $T_1$ and $T_2$, which change the signal intensity of the acquired MR images. The concentration of the agent can be obtained by dynamic measurement of the relaxation rate $\Delta R_1$ ($R_1=1/T_1$) that can be calculated using series of $T_1$ weighted images. Because of the long imaging time for $T_1$ mapping, this method is not practical in most of dynamic MR imaging. In this report, $^{19}$F MRI is presented as an alternative method to access the drug quantity. The concentration of fluorine compound is directly proportional to the $^{19}$F signal in density weighted $^{19}$F-MRI. Strong NMR signal due to the large gyromagnetic ratio, minimal background signal and exquisite sensitivity to changes in the microenvironment have been exploited to design and apply diverse reporter molecules [1]. There are also problems. Firstly, the signal is too low compare to proton signal; secondly, its sensitivity to changes in electron environment causes the signal split and further reduces the signal. To address these problems, a new $^{19}$F based multifunctional drug delivery vehicle (***F***-amphiles) has been developed, which contains 27 fluorine atoms in each molecule and all fluorine nuclei together provide a singlet $^{19}$F signal [2].

**Methods:** A female athymic nu/nu (nude) mouse (32.2 g, Frederick, MD, National Cancer Institute) was used in the animal study. The mouse is about 7 weeks old. In this work, a second generation ***F***-amphile, ($G_2$ ***F***-amphile) is used. The injection of 500 µl $G_2$ ***F***-amphiles (with 64 mmol/kg fluorine) was given through the mouse tail vein. An MRI experiment was performed at 115.92 MHz for $^{19}$F MRI and at 123.24 MHz for $^{1}$H MRI in a Siemens 3T Trio clinical MRI system (Siemens Medical Solution, Erlangen, Germany). A transmit-receive (T/R) solenoid coil was constructed with a dimension of 115 mm length and 70 mm diameter using the active T/R switching with PIN diode. $^{19}$F images were obtained at 20 and 40 minute time points after ***F***-amphiles was injected. A gradient-echo (GRE) pulse sequence was used for $^{19}$F MRI with the imaging parameters; 128x64 acquisition resolution, 20 averages, repetition time (TR) 0.4 s, echotime (TE) 2.98 ms, receiver bandwidth 260 Hz/pixel (or 33 kHz), flipangle 90°, and spatial resolution 1.5×1.5×3.0 mm$^3$. Imaging time was 4 min 20 s. After completion of $^{19}$F MRI at 40 min time point, $^{1}$H MR images were acquired at the same imaging plane and the locations of FMRI using body RF coil and spin-echo pulse sequence with 0.5 s TR, 6.4 ms TE, and spatial resolution of 0.5×0.5×3.0 mm$^3$. The animal stayed in the same location during the entire experiment.

**Results & discussions:** Colored $^{19}$F MR images of three sagittal slices of a mouse were overlaid onto $^{1}$H MR images using the same color scale and the window levels (i.e., brightness and contrast) in Fig. 1. The color bar in each image represents the relative signal intensities of the $^{19}$F NMR signal. The overlaid images in Figs. 1a and 1b clearly demonstrate the different distributions of the substance in different organs, such as heart, liver, kidney, and bladder. The spatial change in the signal intensity between two time points may be used to understand the pharmacokinetics. The mean signal intensities were measured for several regions-or-interest (ROIs) of heart, liver, kidney, and bladder that are indicated in Fig. 1 and plotted in Fig. 2 for two time points. This plot indicates the rapid changes in the heart, liver, and kidney, as shown in Fig. 1. The change of the signal intensity in heart is the greatest, and that of the bladder is almost constant during the time course of 20 minutes. Images of slice 4 indicate that the area of bladder at time 40 min is larger than that of 20 min, which indicates the expansion of the bladder because of the increased accumulation of the urine. The reduction of the signal intensities of different organs between two time points may be related to the whole-body distribution of the compound as well as the excretion at the kidney. The $^{19}$F NMR signals from other organs may be below the detection limit of the hardware. The spatial change of $^{19}$F MRI signal may also be caused by the change in increased $T_1$ relaxation time, because obtained $^{19}$F MR images using TR of 0.4 s may not be density-weighted but $T_1$ weighted. However, it is not likely that the $T_1$ of the compound changed unless the compound breaks between two time points. Further investigation is needed.

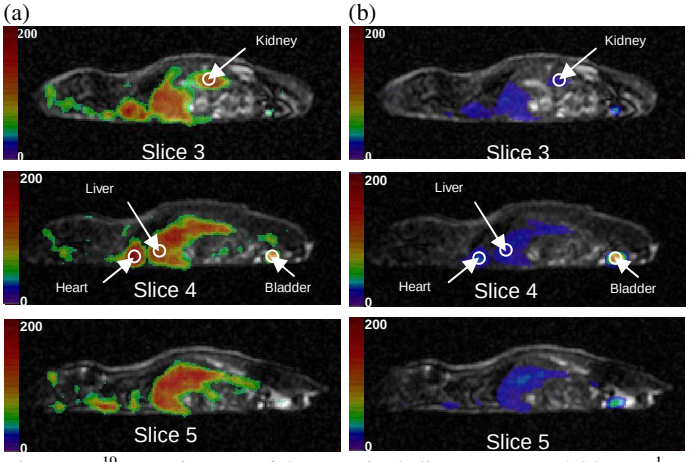


**Figure 1**. $^{19}$F MR images of three sagittal slices were overlaid onto $^{1}$H MRI for (a) 20 minutes and (b) 40 minutes time points. The same window level was used for the overlaid $^{19}$F MRI of both time points.

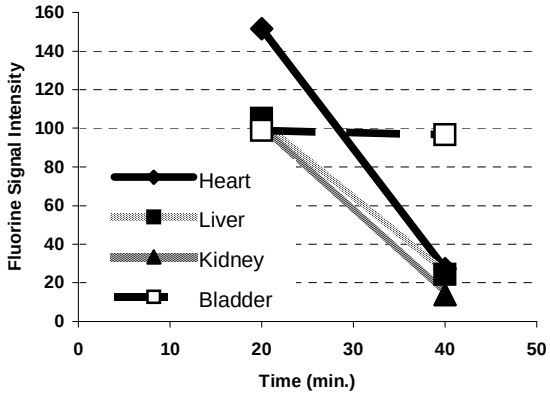


**Figure 2**. Plots of signal intensities of the region of interests (ROIs) for two time points. The locations of the ROIs are indicated in Fig. 1.

**Conclusions:** $^{19}$F based drug delivery vehicle and $^{19}$F MR facility on 3T clinical MR scanner has been developed to image a $^{19}$F labeled compound. Animal experiments have been performed and the preliminary results indicated the encouraging feasibility of $^{19}$F MR in pharmacokinetics and pharmacodynamics research.

**Acknowledgement:** This work was supported by the Margolis Foundation and NIH Grants EY015181 and EB004416.

**References:** [1] J. Yu, etc. Current Med. Chem. 2005, 12, 819. [2] Z. X. Jiang, Y. B. Yu. Tetrahedron 63 (2007) 3982–3988.